PPPL-3279, Preprint: January 1998, UC-420, 426

Toroidal Alfvén Eigenmodes in TFTR Deuterium-Tritium Plasmas

R. Nazikian, G.Y. Fu, Z. Chang, S.H. Batha[1], H. Berk[2],
R.V. Budny, Y. Chen, C.Z. Cheng, D.S. Darrow, N.N. Gorelenkov[3],
F.M. Levinton[4], S.S. Medley, M.P. Petrov[5], M.H. Redi, E. Ruskov, D.A. Spong[6], R.B. White, and S.J. Zweben

Princeton Plasma Physics Laboratory, Princeton, N.J. 08543, USA
[1]Science Research Laboratory, Somerville, MA 02143, USA
[2]University of Texas, Austin, TX 78714, USA
[3]Troitsk Institute of Fusion and Innovative Research, Troitsk, Russia
[4]Fusion Physics &Technology, Torrance, CA 90503, USA
[5]A.F. Ioffe Physical-Technical Institute, St. Petersburg, Russia
[6] Oak Ridge National Laboratory, Oak Ridge, Tennessee

Abstract

Purely alpha-particle-driven Toroidal Alfvén Eigenmodes (TAEs) with toroidal mode numbers n=1-6 have been observed in Deuterium-Tritium (D-T) plasmas on the Tokamak Fusion Test Reactor [D.J. Grove and D.M. Meade, Nucl. Fusion **25**, 1167 (1985)]. The appearance of mode activity following termination of neutral beam injection in plasmas with q(0)>1 is generally consistent with theoretical predictions of TAE stability. [G.Y. Fu et al., Phys. Plasmas **3**, 4036 (1996)] Internal reflectometer measurements of TAE activity is compared with theoretical calculations of the radial mode structure. Core localization of the modes to the region of reduced central magnetic shear is confirmed, however the mode structure can deviate significantly from theoretical estimates. The peak measured TAE amplitude of $\delta n/n \sim 10^{-4}$ at r/a~0.3-0.4 corresponds to $\delta B/B \sim 10^{-5}$, while $\delta B/B \sim 10^{-8}$ is measured at the plasma edge. Enhanced alpha particle loss associated with TAE activity has not been observed.

PACS numbers: 52.55.Fa, 52.35.Bj, 52.35.Py, 52.55.Pi

I. Introduction

Satisfying the dual requirement of good thermal and energetic particle confinement is crucial for an attractive reactor concept. Optimal Deuterium-Tritium (D-T) reactor performance requires that fusion alpha particles be confined on the order of their slowing down time. Enhanced loss of partially thermalized alpha particles from the reactor core may lead to excessive heat load on the first wall and reduction of central alpha heating efficiency. An important goal of the Tokamak Fusion Test Reactor (TFTR) DT program was to investigate the behavior of 3.5 MeV fusion alpha particles under reactor relevant conditions of high toroidal field (B_T~5 T), high plasma temperatures (T_i~20 keV, T_e~10 keV) and central alpha pressure in the range β_α~0.1-0.3% [compared to volume averaged β_α~0.5-1.0% expected in a D-T reactor]. Early theoretical analysis indicated that collective alpha particle phenomena relevant to a D-T reactor may start to be observed for the range of β_α achieved in TFTR. [1]

It has long been known that magnetohydrodynamic (MHD) activity can enhance energetic particle loss, possibly leading to localized heating and damage to plasma facing components. [2] Instabilities collectively excited by large populations of resonant particles are considered to be particularly deleterious to energetic particle confinement. One instability with the potential for strong interaction with energetic alpha particles in a DT reactor is the Toroidal Alfvén Eigenmode (TAE). [3] These modes occur within toroidicity induced gaps in the shear Alfvén spectrum and have received considerable attention in recent years due to their low instability threshold and ability to resonate with alpha particles in a DT reactor. [4]

Initial DT experiments in TFTR showed no indication of TAE activity even with the highest achieved fusion power levels of 10.7 MW [$\beta_\alpha(0)$~0.3%]. These early results on TFTR lead to an intensive modeling effort, which ultimately produced new predictions for further experiments. Motivated by theoretical calculations of reduced instability threshold for alpha-driven TAEs under conditions of low beam ion Landau damping, weak magnetic shear and elevated central safety factor, [5,6,7] recent experiments led to the first observation of purely alpha-particle-driven TAEs in TFTR. [8]

In this paper we update experimental results on alpha-particle-driven TAEs in TFTR. In particular, the internal structure of alpha-driven TAEs is measured for the first time and compared with theoretical calculations of the radial eigenmode structure from the NOVA-K code. [9] Section II presents the basic observation of Toroidal Alfvén Eigenmodes in a range of DT plasmas characterized by varying levels of central q(0) and $\beta_\alpha(0)$. Key factors which identify these modes as TAEs are discussed (frequency, mode number and timing). Statistical analysis of alpha-driven TAEs is presented in section III. In section IV we report the first detailed internal measurements of the radial structure of alpha-particle-driven TAEs in TFTR and compare results with theoretical calculations of the radial eigenfunction from NOVA-K using Motional Stark Effect (MSE) measurements of the q-profile [10] and TRANSP simulation of the alpha particle distribution [11]. Internal measurements confirm the core localization of these modes. However discrepancies arise between the observed and theoretically predicted mode frequency and mode structure for the lowest toroidal mode numbers. Alpha particle loss measurements are present in Section V and results summarized in section VI.

II. Alpha particle driven TAEs in TFTR

The purpose of this section is to present the basic mode observations on TFTR and to indicate that necessary criteria are indeed satisfied for alpha-particle-driven TAE instability. Comparison to linear TAE theory has been published elsewhere. [12]

A. Background

In general, the calculation of TAE stability is very complex and involves a formidable range of possible damping mechanisms including (but not restricted to) thermal/neutral beam ion Landau damping, electron Landau damping, radiative damping due to coupling to kinetic Alfvén waves, continuum damping, etc. [9,13,14] However, the fundamental ingredient for destabilizing these modes is a reservoir of sufficiently energetic particles which can resonate with the mode. For a slowing down distribution of energetic particles, the pressure gradient must exceed a critical value, and

this condition is usually given by $\omega_{*i\alpha} > \omega_{TAE}$, where $\omega_{*i\alpha}$ is the diamagnetic frequency of the energetic ions and ω_{TAE} is the TAE frequency. [15,16]

The mode itself satisfies the dispersion relation for Alfvén waves $\omega_{TAE} = k_{||} V_A$ where $k_{||} \approx 1/2qR$ and $V_A = B/\sqrt{4\pi\rho}$ is the Alfvén velocity, ρ is the ion mass density and B is the magnetic field strength. For passing alpha particles to resonate with the TAE, the condition $V_\alpha \approx V_A$ and/or $V_A/3$ must be satisfied, whereas for trapped particles, the precession frequency must match the mode frequency. In a DT reactor, the birth velocity of alpha particles $V_\alpha = \sqrt{2E_\alpha/m_a} \approx 1.3 \times 10^9$ cm.s^{-1} will be close to the Alfvén velocity, so that these particles can resonate with TAEs and possibly lead to enhanced alpha particle loss. However the same resonance condition can lead to damping by thermal and neutral beam ions when their diamagnetic frequency is well below the TAE frequency. [9] In a typical high performance hot ion mode plasma on TFTR the thermal and beam ion diamagnetic frequencies are of the order 10-20 kHz in the core for toroidal mode number n=1, and the beam ion birth velocity is close to the sideband resonance condition $V_A/3$, satisfying the condition for mode damping.

For typical TFTR DT plasmas the alpha particle diamagnetic frequency can exceed 1 Mhz for toroidal mode numbers n>1 and this can be maintained up to 300-400 ms after termination of neutral beam injection, compared to the characteristic TAE frequency which is in the range 150-250 kHz. Because of the rapid slowing down of neutral beam ions relative to the alpha particles, it was recognized early on that optimal conditions for observing TAEs in TFTR would be 100-200 ms after termination of neutral beam injection. [11,14] The non-observation of TAEs even in the afterglow of the highest fusion power plasmas with $\beta_\alpha(0) \sim 0.3\%$ indicates that factors other than beam and ion Landau damping were affecting mode stability.

Based on these early TFTR results, theoretical analysis indicated that the reducing central magnetic shear and raising q(0) to align low-n modes with the peak in the alpha particle pressure gradient would excite the TAE in TFTR following the termination of DT beam injection. [6,7] In particular, the damping on kinetic Alfvén waves (radiative damping) decreases with increasing mode width and decreasing magnetic shear. [13] Raising q(0)>1 to

align low-n gaps to the peak of the alpha pressure gradient also reduces radiative damping due to its toroidal mode number dependence.

B. Observations

By using full radius plasmas during current ramp-up on TFTR the central safety factor can be raised above 1 and broad regions of reduced central magnetic shear in the plasma core can be obtained. Purely alpha-particle-driven TAEs were first observed on TFTR using this plasma startup procedure. [8] Alpha-driven TAEs have only been observed in a transient phase 100-300 ms following the end of DT neutral beam injection in reduced magnetic shear DT-plasmas on TFTR.

Figure 1 shows time traces of relevant plasma parameters for a DT plasma in which TAE activity is observed. Theory indicates that thermal and beam ion Landau damping are dominant stabilizing terms during high power neutral beam injection, so that the only window for observing TAEs is in the narrow time slice following the end of beam injection. [6] The beam ion velocity is usually very close to $V_A/3$, which is expected to strongly damp the mode via the sideband resonance. Typical Deuterium or Tritium beam ion slowing down times are of order 80-100 ms. The decay of the plasma beta occurs on a similar time scale, as indicated by the trace of the central plasma beta in Fig. 1. However, energetic alpha particles have a slowing down time considerably longer (300-500 ms depending on the plasma conditions in the afterglow) as indicated by the β_α trace in Fig. 1. Thus, one of the key factor in exciting TAEs in TFTR is the decay of the plasma beta on a time scale short compared to the alpha particle slowing down time.

The mode activity is clearly seen after termination of neutral beam injection as indicated by the amplitude of magnetic fluctuations. A sequence of short bursts 50-100 ms in duration are observed with toroidal mode numbers ranging from n=2-4. At the time of mode activity $q(0)\approx 1.5$ as obtained from Motional Stark Effect measurements [17], and $\beta_\alpha(0)\sim 0.05\%$ obtained from TRANSP code kinetic analysis [11]). TRANSP calculates the alpha distribution from the measured neutron rate and profile, using a Monte Carlo analysis with collisional slowing down. Mode activity appears after the slowing down of neutral beam ions (τ_{Beam}~80-100 ms) but before the

thermalization of 3.5 MeV alphas (τ_α~300-400 ms), and in the TAE range of frequency: f_{TAE}~200-250 kHz. The level of magnetic activity observed at the plasma edge is typically very small ($\delta B/B \sim 10^{-8}$), however the internal level of magnetic fluctuations as inferred from reflectometer measurements of the density is considerably higher. Recent theoretical analysis shows that alpha-driven TAEs should indeed be unstable in these discharges in the period 100-300 ms following the termination of neutral beams. [8,12]

As indicated earlier, elevated safety factor and reduced central shear are necessary for exciting alpha-driven TAEs in TFTR. Figure 2 shows q(r) and β_α profiles 150 ms after neutral beam injection for three cases of interest corresponding to a standard supershot with no observed TAE, and two discharges with q(0)~1.5 and q(0)~1.9 for which TAE activity is observed. Note that the highest q(0) plasma has $\beta_\alpha(0)$~0.025% compared to 0.17% for the supershot case. In cases (I) and (ii) q(a)≈4.8, while q(a)≈7.6 in (iii). The magnetic shear at r/a≈0.3 is ~0.3 for the supershot case, ~0.2 for the high q(0) case and ~0.1 for the case with q(0)≈1.5. Figure 3 shows contours of constant magnetic signal level as a function of frequency and time in the first 300 ms following termination of neutral beam injection for the three discharges in Fig. 2. Fig. 3(a) corresponds to the lowest β_α case with the highest q(0) of Fig. 2. Shown are a sequence of n=2,4,3 bursts up to 300 ms after the end of beam injection. TRANSP calculates β_α~0.01% at the time of the last observed mode with an alpha particle diamagnetic frequency > 1 Mhz for n=3. This is consistent with theoretical estimates of the minimum β_α required to destabilize TAEs in the afterglow of high q(0) plasmas in TFTR. [8] Note that the TAE frequency evaluated at r/a=0.3 increases in time due to the decreasing plasma density after the end of neutral beam injection. Each mode chirps up in frequency, consistent with an increasing Alfvén velocity. Also shown for reference is the edge Alfvén frequency relevant to the Alfvén Frequency Mode (AFM) [$f_{AFM}=V_A(q=0.95)/qR$]. [18] This edge localized quasi-coherent AFM is ubiquitous to all discharges, ohmic, deuterium and DT, with an amplitude which scales with the edge density. It is most easily seen in high power supershot plasmas such as in Fig. 3 (c). Fig. 3(b) shows a sequence of bursts in the discharge with q(0)~1.5. Note that the n=2 mode frequency falls somewhat below the TAE frequency. We will return to this mode later when discussing the internal structure of alpha-driven TAEs. Fig. 3(c) for the

q(0)<1 supershot discharge shows no indication of TAE activity although the AFM is clearly visible throughout the period of beam injection and into the afterglow.

A necessary criterion for these modes to be TAEs is that their frequency falls into the toroidicity induced gap in the shear Alfvén spectrum. Shown in Fig. 4 is the gap structure calculated using NOVA-K for the n=4 mode in Fig. 3(b) at t=2.92 sec. Clearly the gaps are all radially very well aligned and the frequency sits in the gap. The core localized gap at r/a≈0.35 resides in the region of weak central shear with a large separation to the next gap position at r/a≈0.6. Under these conditions, theory predicts the core localized TAEs (localized to the region around a single gap) will be most unstable in TFTR DT plasmas. In general, the observed mode frequency falls within the gap width, with the exception of the n=2 mode. The largest uncertainty in the gap position arises from the uncertainty in the measured q-proifle which is around 5-10% for q(0)~1.0 and increases to ~20% for q(0)~2.0.

III. Statistical analysis

In this section we attempt to address general or common characteristics of all the data collected on alpha-driven TAEs in TFTR, as opposed to the detailed analysis of individual discharges when making detailed comparison to theory. Figure 5 shows the distribution of the measured mode frequency compared to the TAE frequency at r/a=0.3 for all the collected data. The TAE frequency is estimated using TRANSP with actual MSE measured q-profiles. An interesting characteristic of the data is that the lowest toroidal mode numbers (n=1 and n=2) consistently fall below the TAE frequency by ~ 30%. Generally, the n=4,5,6 modes agree very well with the estimated TAE frequency, with the n=3 mode falling somewhere between the two cases. Plasma diamagnetic effects or rotation are insufficient to explain this frequency discrepancy. In the afterglow of the discharge, toroidal rotation is entirely negligible due to the absence of applied torque, and the bulk ion diamagnetic frequency is below 10 kHz for n=2. Nonetheless, the frequency of the n=1 and n=2 modes increase with decreasing density in the afterglow as expected for Alfvén modes.

Figure 6 shows the calculated $\beta_\alpha(0)$ vs q(r/a=.3) in DT plasmas with and without TAE activity. The radius r/a=0.3 is used as this corresponds to the gradient region of the alpha distribution where theory predicts unstable modes. [6,7] The threshold β_α can be very low for excitation of TAEs after termination of neutral beams, and appears to be below 0.01% in weak central shear plasmas, consistent with theoretical estimates in similar weak shear discharges. [8] For hot ion mode plasmas with monotonic q-profiles we have $q(.3)<1.4$ and no observed TAEs with $\beta_\alpha \sim 0.2\%$. Note that for the highest β_α supershot plasmas, $q(.3)\sim 1$. In this case the dominant toroidal mode numbers are expected to be high (>5) with strong radiative damping. [6]

Finally, the question of continuum damping and the critical pressure gradient for stabilizing the modes is addressed. An important question is whether the TAE frequency is in the gap during beam injection or whether it is forced into the continuum by the pressure gradients in hot ion mode plasmas. If the latter were true, then the TAE could not be excited during beam injection, even in the absence of thermal and beam ion landau damping. The simplified local theory for TAEs indicates that the critical beta for stabilizing core localized modes is given by $\alpha>\alpha_c$, where $\alpha=2(Rq^2/B^2)dp/dr$, $\alpha_c=3\varepsilon+s^2$, and ε is the inverse aspect ratio. [6,9] It is interesting to note that reducing magnetic shear and increasing q tends to reduce the pressure gradient required to stabilize the modes. An important consideration in originally designing these experiments was whether α would fall below α_c fast enough for the alpha particles to excite the mode after termination of DT neutral beams. Figure 7 shows α vs α_c at r/a=0.3 at the end of beam injection and during observed TAE activity in the afterglow. These parameters were calculated from TRANSP using measured pressure and q-profiles. It would appear from the local analysis that continuum damping of the modes is only significant at the highest achieved pressures in these experiments, and that the mode is most likely in the gap during beam injection and stabilized by other damping terms such as beam ion Landau damping. Unfortunately, the statistical variation of the ratio $V_b/3V_A$ (~0.9-1.1, where V_b is the beam velocity) is not sufficient to determine experimentally the relative importance of beam damping vs radiative and other damping terms during beam injection.

IV. Radial structure of alpha-particle-driven TAEs

Internal measurements of alpha-driven TAEs were obtained using the X-mode core reflectometer diagnostic on TFTR. [19-22] This diagnostic measures phase fluctuations induced on a probing microwave beam reflected from density variations in the plasma. In this paper we use the assumption of one dimensional geometric optics for the perturbed phase of the reflected microwave beam,

$$\tilde{\varphi} \approx 2k_0 \int \sqrt{\varepsilon_0 + \tilde{\varepsilon}}\, dz - 2k_0 \int \sqrt{\varepsilon_0}\, dz$$

where ε_0 is the unperturbed permittivity of the plasma for X-mode propagation, $\tilde{\varepsilon}$ is the perturbed permittivity due to density fluctuations, k_0 is the microwave radial wavenumber in vacuum, $\tilde{\varphi}$ is the perturbed phase of the reflected microwaves and the integration extends from the plasma edge (ε_0=1) to the cutoff layer where ε_0=0. This relation holds so long as the plasma perturbation (such as TAEs) has a wavelength much longer than the wavelength of the probing microwaves. Although the integral starts from the plasma edge, the dominant contribution to $\tilde{\varphi}$ occurs near the reflecting layer.

A plot of the radial variation of the microwave reflecting layer (ε_0=0) as a function of the launch frequency is shown in Fig. 8 for a typical plasma with alpha-driven TAEs. A unique advantage of using the upper X-mode reflection in most tokamaks is that it allows access to the high field side of the magnetic axis for waves launched on the outer midplane. This is due to the strong dependence of the cutoff position on the radially decreasing toroidal field strength. A radial scan of the mode structure can be obtained using the three fixed frequency channels (170 Ghz, 143 Ghz and 135 Ghz) on TFTR by introducing a small (10%) variation in the toroidal field strength keeping q(a) constant. By this procedure, radial scans of the eigenmode structure can be obtained using a succession of plasmas with reproducible mode activity as measured on external Mirnov coils.

Reproducible plasma conditions were obtained for the q(0)~1.5 plasmas with q-profile shown in Fig. 2. A simulation of the reflectometer response vs reflecting layer position is shown in Fig. 9 for n=2 and n=4 eigenfunctions

obtained from NOVA-K analysis. [9,12] It is apparent that the ballooning structure of the eigenfunctions as calculated by NOVA-K is well reproduced by the simulated reflectometer measurements. A basic prediction of TAE theory is that the alpha driven TAEs in TFTR are core localized and ballooning, i.e. that the modes are largest on the low field side of the magnetic axis and localized to the region of weak central shear.

A surprising result from the reflectometer measurements is that the structure of the low frequency n=2 mode in Fig. 5 and Fig. 3(b) is strongly anti-ballooning, counter to the predicted eigenfunction shown in Fig. 9. Figure 10 displays four signals, three from the reflectometer and one from the Mirnov coil situated on the outer midplane. One of the reflectometer channels is on the high field side of the magnetic axis while the other two channels are on the low field side. The reflectometer measurements clearly indicate a dominant n=2 mode on the high field side of the magnetic axis, but there is no indication of n=2 activity on the two other reflectometer channels. Although the n=2 is clearly larger on the high field side of the axis at r/a=-0.36, it has a lower amplitude on the Mirnov coil on the outer midplane as compared to the n=4 mode. This is qualitatively consistent with reflectometer measurements which indicate that the n=4 mode is dominant on the outer midplane. Note also that the in/out structure of the n=4 mode appears to be evolving as the magnetic signal increases on the outer midplane.

Collecting *all* available data on the n=2 mode, Fig. 11 shows the fit to the reflectometer data using a model Gaussian density perturbation located at r/a= +/-0.32. Note that the n=2 mode is identified from measurements taken on the toroidal array of Mirnov coils while the internal structure is determined from the radial array of reflectometer measurements at one toroidal location. The reflectometer data is consistent with an anti-ballooning mode structure with a peak amplitude $\delta n/n \sim 1.5 \times 10^{-4}$, which corresponds to a peak magnetic field fluctuation level $\delta B/B \sim 1.5 \times 10^{-5}$. [8] This should be compared to the peak magnetic signal on the outer midplane of $\sim 2 \times 10^{-9}$ for the n=2 mode. This result clear indicates the core localization of the mode. The anti-ballooning structure contrasts with that expected theoretically from Fig. 9(b). Furthermore, the low mode frequency is also at variance with theoretical

expectations which would put the n=2 TAE frequency close to the measured n=4 frequency.

Figure 12 displays the normalized mode frequency and magnetic signal level of the n=4 mode vs time for six discharges for which reproducible n=4 activity was obtained and for a range of toroidal field strengths with constant q(a). The frequency normalization ($f \bullet \sqrt{n}/B$) takes into account any variation of the toroidal field and plasma density among the discharges. Two of the signals have been scaled in amplitude by a factor x0.75 in order to bring them into the range of the other signals. The reflectometer phase measurements for these two discharges have also been scaled by the same factor.

Figure 13 compares the radial mode structure of the n=4 mode at 90% of the peak magnetic signal (Fig. 13b) with the radial mode structure at the time of half the peak of the magnetic signal (Fig. 13b). The hint of a changing radial mode structure indicated by Fig. 10 is indeed revealed from the reflectometer measurements taken over a range of discharges. Early in the mode evolution (Fig. 13a) the n=4 mode is roughly symmetric on the high and low field side of the magnetic axis, but transforms into an outward ballooning structure at the end of the mode duration shown in Fig. 13b. The core localization, narrow width and frequency of the n=4 mode are generally consistent with core localized TAEs predicted by theory and shown in Fig. 9. However the changing radial symmetry of the mode is difficult to explain using current TAE theory which predicts only outward ballooning modes should be unstable.

The density fluctuation level of all these modes are small ($\delta n/n \sim 0.6\text{-}0.8 \times 10^{-4}$) and corresponds to $\delta B/B \sim 10^{-5}$ as estimated from theoretical calculations of the radial eigenfunction. Note that the peak fluctuation level does not vary significantly at the two times of interest at the beginning and end of the mode burst on the outer midplane Mirnov coil, even though the magnetic signal level changes almost 100%. This suggest an evolving internal mode structure, where the TAE progressively becomes radially more ballooning and couples more strongly to the plasma edge before dissipating. It is unclear whether this evolution is determined by the non-linear interaction of the alpha particles with the mode or whether it is due to changing plasma

conditions such as an evolving q-profile. Preliminary analysis indicates that the peak density fluctuation level is of the order expected from non-linear theory for single mode saturation. [23] A detailed non-linear analysis will be presented in a future publication.

V. Alpha loss measurements

At present no alpha particle loss has been observed on the lost alpha detectors, consistent with the weak mode amplitudes. [24] Figure 14 illustrates a typical orbit of a 2 MeV alpha particle near the trapped/passing boundary which intercepts the midplane lost alpha probe and the region where the TAEs are located. For weak mode amplitudes the dominant loss is expected to be near the trapped counter-passing boundary. [25] Particles need only lose a small amount of their energy to the mode to fall into these barely trapped orbits and escape from the plasma. Figure 15 shows the time history of the neutron rate, alpha flux to the midplane probe and the time history of the magnetic signals on the outer midplane, showing no evidence of enhanced alpha loss on any of the lost alpha detectors. One possible reason for this is that the alpha particles near the trapped passing boundary may be lost before the mode activity appears. On the other hand there is some evidence for the internal redistribution of confined deeply trapped alpha particles in the presence of even weak alpha-driven TAEs with $q(0)>2$. [26] These results are currently being examined numerically using the ORBIT guide center code. [27,28]

VI. Summary

In this paper we reported on recent developments in our understanding of alpha-particle-drive Toroidal Alfvén Eigenmodes in TFTR. Purely alpha-particle-driven Toroidal Alfvén Eigenmodes (TAEs) with toroidal mode numbers n=1-6 have been observed in DT plasmas after the termination of neutral beam injection. These observations are in general agreement with theoretical predictions for the excitation of alpha-driven TAEs. Internal reflectometer measurements of TAE activity was obtained using the X-mode reflectometer diagnostic. These measurements reveal the core localization of the modes to the region of reduced magnetic shear. The peak measured TAE

amplitude of $\delta n/n \sim 10^{-4}$ at r/a~0.3-0.4 corresponds to $\delta B/B \sim 10^{-5}$, while $\delta B/B \sim 10^{-8}$ is measured at the plasma edge. However the radial structure and particularly the ballooning character of the n=2 mode differs significantly from theoretical predictions for alpha-driven TAEs. Enhanced alpha particle loss associated these modes has not been observed.

Acknowledgments

Research sponsored by the Office of Fusion Energy Sciences, U. S. Department of Energy, under contract DE-AC02-CH0-3073.

References

[1] C.Z. Cheng, G.Y. Fu, H.E. Mynick et al., Plasma Physics and Controlled Nuclear Fusion Research 1992 (Proc. 14th Int. Conf. Montreal, 1992), Vol. 2, IAEA, Vienna (1999) 51.

[2] J.D. Strachan, S.J. Zweben, C.W. Barnes, et al., in Plasma Physics and Controlled Nuclear Fusion Reseasch 1988 (Proc. 12 Int. Conf. Nice, 1988), Vol. 1, International Atomic Energy Agency, Vienna (1989) 257.

[3] C.Z. Cheng and M.S. Chance, L. Chen and M.S. Chance, Ann. Phys. (NY) **161**, 21 (1985).

[4] G.Y. Fu and J.W. Van Dam, Phys. Fluids B **1**, 1949 (1989).

[5] R.V. Budny, M.G. Bell, H. Biglari et al., Nucl. Fusion **32**, 429 (1992).

[6] G.Y. Fu, C.Z. Cheng, R.V. Budny et al., Phys. Rev. Lett. **75**, 2336 (1995).

[7] D. Spong, C.L. Hedrick, B.A. Carreras et al., Nucl. Fusion **35**, 1687 (1995).

[8] R. Nazikian G.Y. Fu, S.H. Batha et al., Phys. Rev. Lett. **78**, (1997) 2976.

[9] G.Y. Fu, C.Z. Cheng, R.V. Budny et al., Phys. Plasmas **3** (1996) 4036.

[10] F.M. Levinton, R.J. Fonk, G.M. Gammel et al., Phys. Rev. Lett. **63**, 2060 (1989).

[11] R.V. Budny, M.G. Bell, A.C. Janos et al., Nucl. Fusion **35**, 1497 (1995).

[12] G.Y. Fu, R. Nazikian, Z. Chang et al., proceedings of the 5th IAEA Technical Committee Meeting on Alpha Particle Physics, September 8-11 1997 Abingdon, UK. (Internationa Atomic Energy Agency, Vienna.)

[13] R. Mett and S. Mahajan, Phys. Fluids B **4**, 2885 (1992).

[14] S.J. Zweben, R.V. Budny, C.Z. Cheng et al., Nuc. Fusion **36**, 987 (1997).

[15] M.N. Rosenbluth and P.H. Rutherford, Phys. Rev. Lett. **34**, 1428 (1975).

[16] G.Y. Fu and C.Z. Cheng, Phys. Fluids B, **4** (1992) 3722.

[17] S.H. Batha, F.M. Levinton, S.P. Hirshman, M.G. Bell, R.M. Wieland, Nucl. Fusion **36** (1996) 1133.

[18] Z. Chang, E.D. Fredrickson, S.J. Zweben et al., Nucl. Fusion **35** (1995) 1469.

[19] E. Mazzucato and R. Nazikian Phys. Rev. Lett. **71**, (1993) 1840.

[20] R. Nazikian Z. Chang, E.D. Fredrickson et al., Phys. Plasmas **3**, (1996) 593.

[21] R. Nazikian and E. Mazzucato Rev. Sci. Instrum **66**, (1995) 392.

[22] R. Nazikian, R. Majeski, E. Mazzucato et al., Rev. Sci. Instrum. **68**, (1997) 450.

[23] B.N. Breizman, H.L. Berk, M.S. Pekker, F. Porcelli, G.V. Stupakov, K.L. Wong et al., Phys. Plasmas **4** 1559 (1997).

[24] D. Darrow, S.J. Zweben, Z. Chang et al., Nuc. Fusion **37,** (1997) 939.

[25] D.J. Sigmar C.T. Hsu, R.B. White and C.Z. Cheng, Phys. Fluids B **4**, 1506 (1992).

[26] M.P. Petrov, R.V. Budny, Y. Chen et al., proceedings of the 5th IAEA Technical Committee Meeting on Alpha Particle Physics, September 8-11 1997 Abingdon, UK. (Internationa Atomic Energy Agency, Vienna.)

[27] R.B. White, E.D. Fredrickson, D. Darrow, M. Zarnstorff, R. Wilson, S. Zweben, K. Hill, Y. Chen, and G.Y. Fu, Phys. Plasmas **2** 2871 (1995).

[28] M. H. Redi, R. B. White, S. H. Batha, F. M. Levinton, D. C. McCune, Phys. Plasmas, **4**, 4001 (1997).

Figure Captions

Figure 1 - Evolution of (a) DT neutral beam power, (b) central β_α, (c) central plasma beta, (d) central q(0) obtained from MSE and (e) amplitude envelope of edge magnetic fluctuations on outer midplane. Plasma parameters during mode activity are: (#103101) B_T=5.T, I_p=2.0 MA, R=2.52 m, $n_e(0)$=4.3 x 10^{19} cm^{-3}, $T_e(0)$=6 keV, $T_i(0)$=15 keV. Shaded region denotes time of TAE. Mode activity appears after the slowing down of neutral beam ions (τ_{Beam}~80-100 ms) but before the thermalization of 3.5 MeV alphas (τ_α~300-400 ms), and in the TAE range of frequency: f_{TAE}~200-250 kHz.

Figure 2 - Profiles of (a) β_α and (b) q(r) for three different DT plasmas ~150 ms following turn off of neutral beam heating. These plasmas have varying levels of TAE activity. The highest β_α in curve (I) corresponds to a high performance hot ion mode plasma with q(0)<1 and no alpha driven TAEs. Curves (ii) and (iii) are for reduced central magnetic shear DT plasmas with lower β_α than (I) but with observed TAE activity after the termination on neutral beam heating. Plasmas parameters for (I) and (II) are the same as in the caption of Fig. 1. Parameters for (III) with q(0)~2 at ~150 ms following the end of DT neutral beams are : B_T=5.3 T, I_p=1.6 MA, R=2.60 m, P_{NBI}= 26 MW, P_{fus}=2.5 MW, $n_e(0)$=3.5x10^{19} cm-3, $T_e(0)$=5.3 keV, and $T_i(0)$= 10 keV.

Figure 3 - Evolution of magnetic fluctuations vs. frequency and time after termination of neutral beam injection for the three plasmas in Fig. 2. Overlaid are the AFM frequency at the plasma edge and the TAE frequency at r/a=0.3. No TAEs are seen in (a) corresponding to the high performance q(0)<1 plasma in Figure 2 (I) with $\beta_\alpha(0)$~0.15%. However the edge localized quasi-coherent AFM is observed. In (b) [corresponding to the q(0)~1.5 plasma of Fig. 2 (II)] a sequence of TAEs with mode numbers from n=2-5 are observed following the end of neutral beam injection. In (c) [corresponding to the q(0)~1.8 plasma of Fig. 2 (II)] a sequence of three modes are observed up to 300 ms following termination of DT neutral beam injection.

Figure 4 - Toroidicity induced n=4 gap in the shear Alfvén spectrum for the case of Fig. 3 (b) at the time of the n=4 mode activity. The gap structure is radially well aligned and the mode frequency (marked by the dashed line)

occurs in the gap as expected for TAEs. Note that the n=2 mode of Fig. 3 (b) appears to be below the bottom of the gap. The dominant uncertainty in the gap frequency arises from the uncertainty in the central safety factor obtained from MSE measurements ($\omega \sim V_A/q$). For q(0)~1.0, the uncertainty is ~10% and increases to ~20% for q(0)~2.0. Nonetheless, it is difficult to make both mode frequencies fit into the gap width.

Figure 5 - Observed frequency on Mirnov coils plotted against the estimated TAE frequency at r/a=0.3 as evaluated from TRANSP using MSE measured q-profiles. The lines represent linear fits to the data for each toroidal mode number from n=2 to n=6. The n=2 and n=1 modes occur ~30 % below the estimated TAE frequency.

Figure 6 - Central $\beta_\alpha(0)$ vs q at r/a=0.3 taken ~150 ms following the end of neutral beam injection. Open circles refer to plasmas with no TAE activity, while closed circles refer to plasmas with observed TAEs. The open circles to the left are all for supershot plasmas. The uncertainty in q from MSE measurements and uncertainty in the estimated β_α from TRANSP analysis is shown. The alpha particle birth rate is calculated from the measured 14 MeV neutron emission profile and classical slowing down on the thermal plasma is assumed.

Figure 7 - Plot of α vs α_{crit} evaluated at r/a=0.3 for all discharges where TAEs are observed. The TAE frequency should occur in the toroidicity induced gap when $\alpha < \alpha_{crit}$. Open circles refer to the time at the end of neutral beam injection when no TAEs are observed, while closed circles are for ~150 ms following DT beam injection when mode activity occurs. The dominant uncertainty arises from the error in the q-profile measurements which is no more than 5-10 % at r/a=0.3, although it increases towards the magnetic axis.

Figure 8 - Right hand X-mode cutoff frequency f_{rx} vs major radius ~150 ms following termination of beam injection at the time of observed mode activity (#103101). Also shown are the plasma frequency f_{pe}, and the first and second harmonic cyclotron frequencies f_{ce}. The arrow indicates the direction of launched waves, which are reflected from the plasma and carry information on internal density fluctuations.

Figure 9 - Simulation of reflectometer measurement (solid line) of TAE radial eigenfunction obtained from the NOVA-K code (dashed) for (a) an n=4 mode and (b) an n=2 mode. [12] Simulation indicates that the general structure of the mode should be well reproduced by the reflectometer measurement.

Figure 10 - Time evolution of the phase observed on the reflectometer channels at (a) r/a=-0.36, (b) r/a=0.25, (c) r/a=0.44, compared to (d) the amplitude of magnetic fluctuations observed on the outboard midplane. Note that the reflectometer does not observe n=2 activity on the low field side of the magnetic axis, consistent with the relatively weak magnetic fluctuation level of the n=2 signal on outboard midplane.

Figure 11 - (a) Map of the phase magnitude observed on the reflectometer (open circles) for the n=2 mode taken over a range of similar plasmas with ~10% variation in toroidal field keeping q(a) constant. These plasmas showed identical TAE activity. In (b) the simulation of the reflectometer response (solid line) to two Gaussian density perturbations (dashed) centered at r/a=0.32 with half width of r/a=0.1. The simulation is also shown in (a) overlaying the reflectometer data. The radial mode structure of low frequency n=2 mode is clearly anti-ballooning.

Figure 12 - Normalized mode frequency (a) and mode amplitude on the outboard midplane Mirnov pickup coil (b) for the n=4 mode vs time for six discharges, following termination of DT neutral beam injection. The shot to shot reproducibility is very good after normalizing out the Alfvén frequency dependence on magnetic field strength and central density. The data represents a reproducible set of mode observations obtained by varying the toroidal field strength from BT=4.5-5.3 T, keeping q(a) constant. In two of the discharges, the mode amplitude was scaled by 0.75 in order to bring it into the range of amplitude of the other discharges.

Figure 13 - Plot of the phase magnitude obtained from local reflectometer measurements taken over all the discharges in figure 12. (a) corresponds to the phase magnitude of the reflectometer measurements taken at the time of

half peak magnetic signal on the rise of the data in Fig. 12, while (b) corresponds to the reflectometer phase level measured at the time corresponding to 90% of the peak of the decaying magnetic signal in Fig. 12. The error bar denotes the uncertainty in the measured phase magnitude determined purely by the signal to noise ratio of the phase spectrum. The shot-to-shot phase variation at a single radial location cannot be determined as each shot represents a different radial location for the reflectometer measurements. The solid line is the simulated reflectometer response to two Gaussian density perturbations located at r/a=0.35 in (a) and r/a=0.45 in (b). The model Gaussian density perturbations are indicated by the dashed curves with axis to the right. The data confirms the core localization of the modes to the region of weak central magnetic shear and also confirms the changing ballooning structure of the mode.

Figure 14 - Plot of the orbit of a 2.0 MeV alpha particle near the couter-passing trapped orbit boundary evaluated at the time of observed mode activity. The orbit intersects both the location of the measured TAEs and the location of the lost alpha probe.

Figure 15 - (a) neutron flux, (b) alpha signal from the lost alpha probe and (c) magnetic fluctuations. No evidence for enhanced alpha loss is observed during the period of TAE activity.

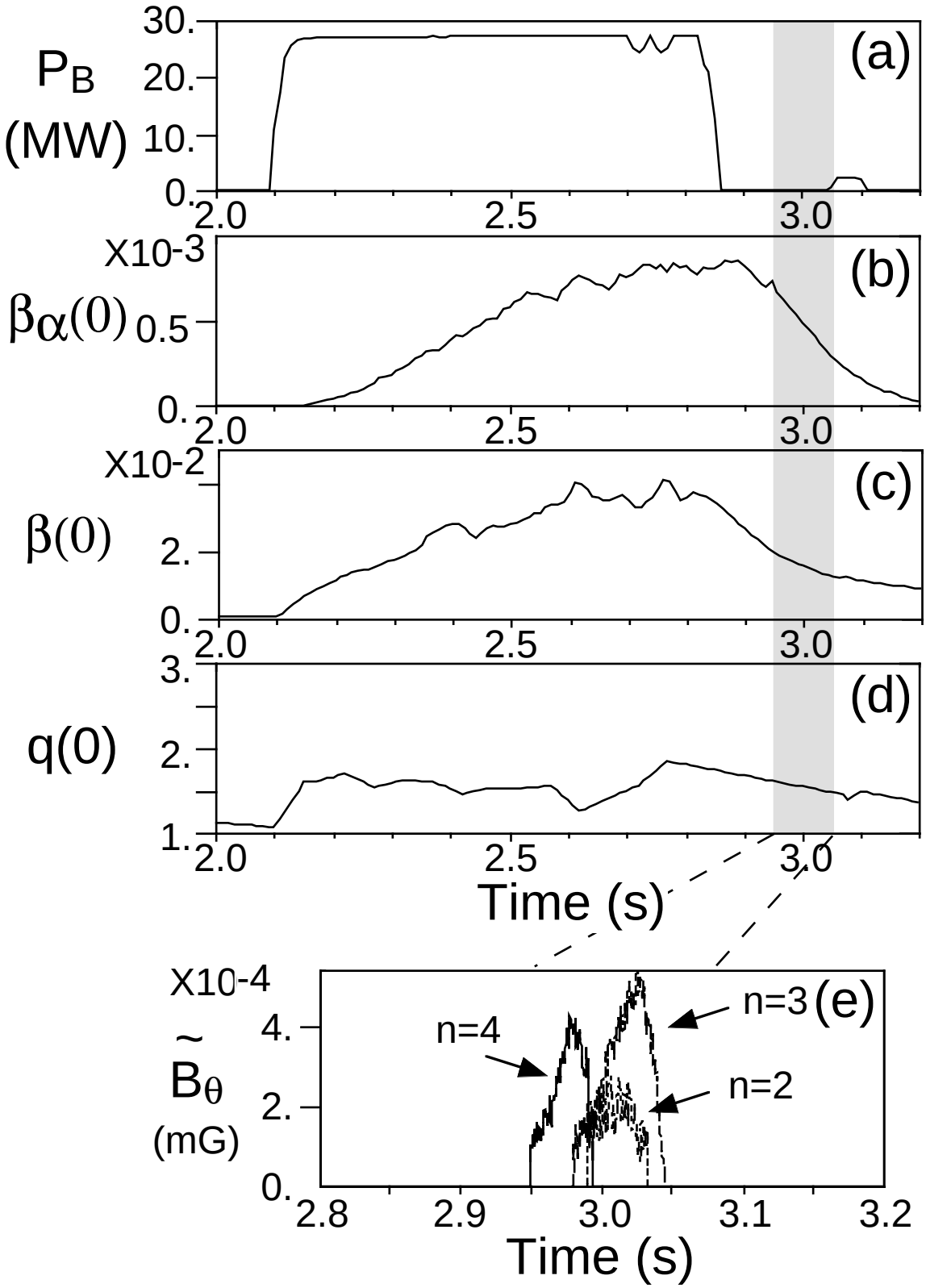

102993a02

PPPL-3279/Figure 1

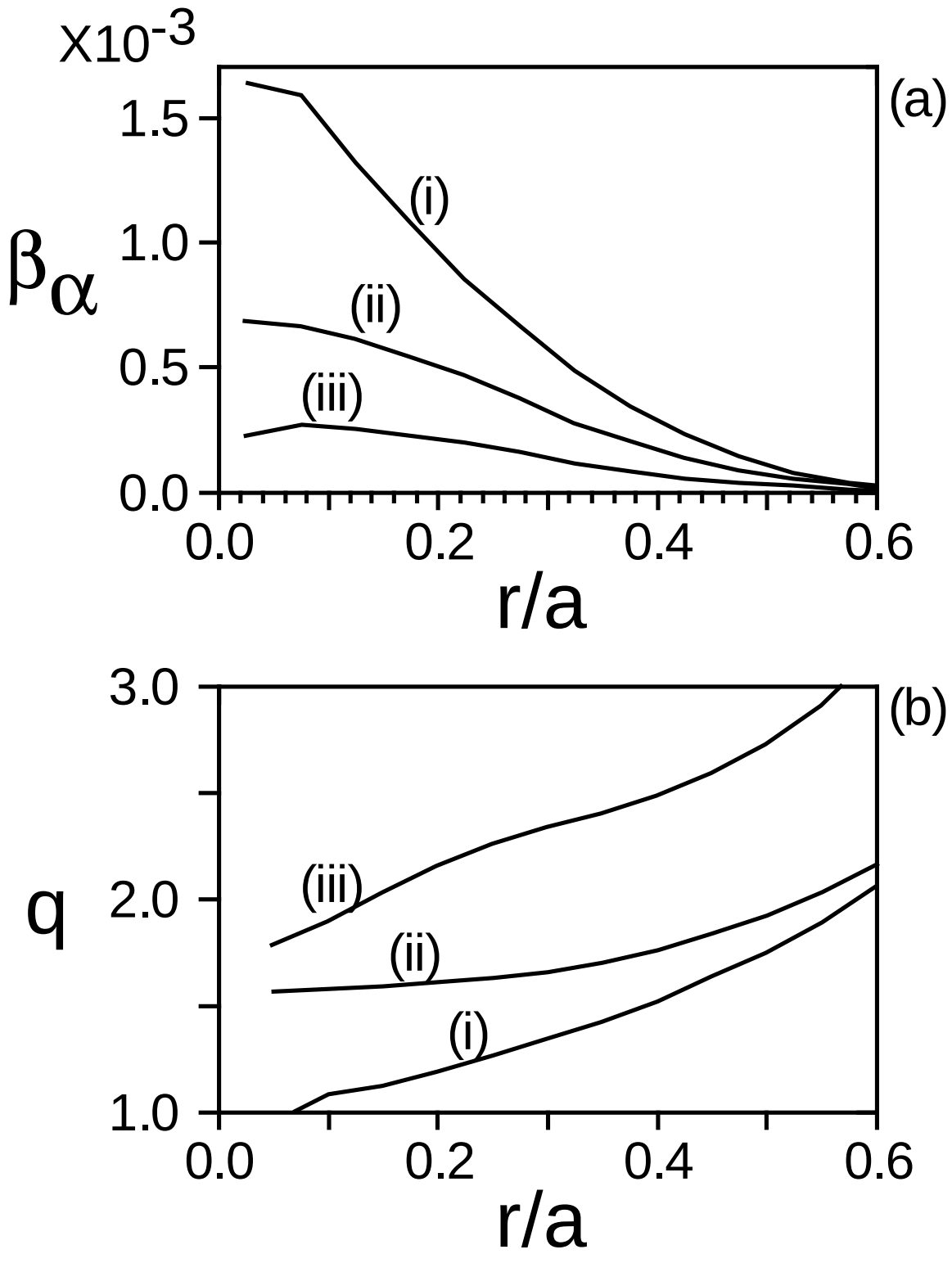
X10-3
1.5
1.0
0.5
0.0
βα
(a)
(i)
(ii)
(iii)
0.0
0.2
0.4
0.6
r/a
3.0
2.0
1.0
q
(b)
(iii)
(ii)
(i)
0.0
0.2
0.4
0.6
r/a

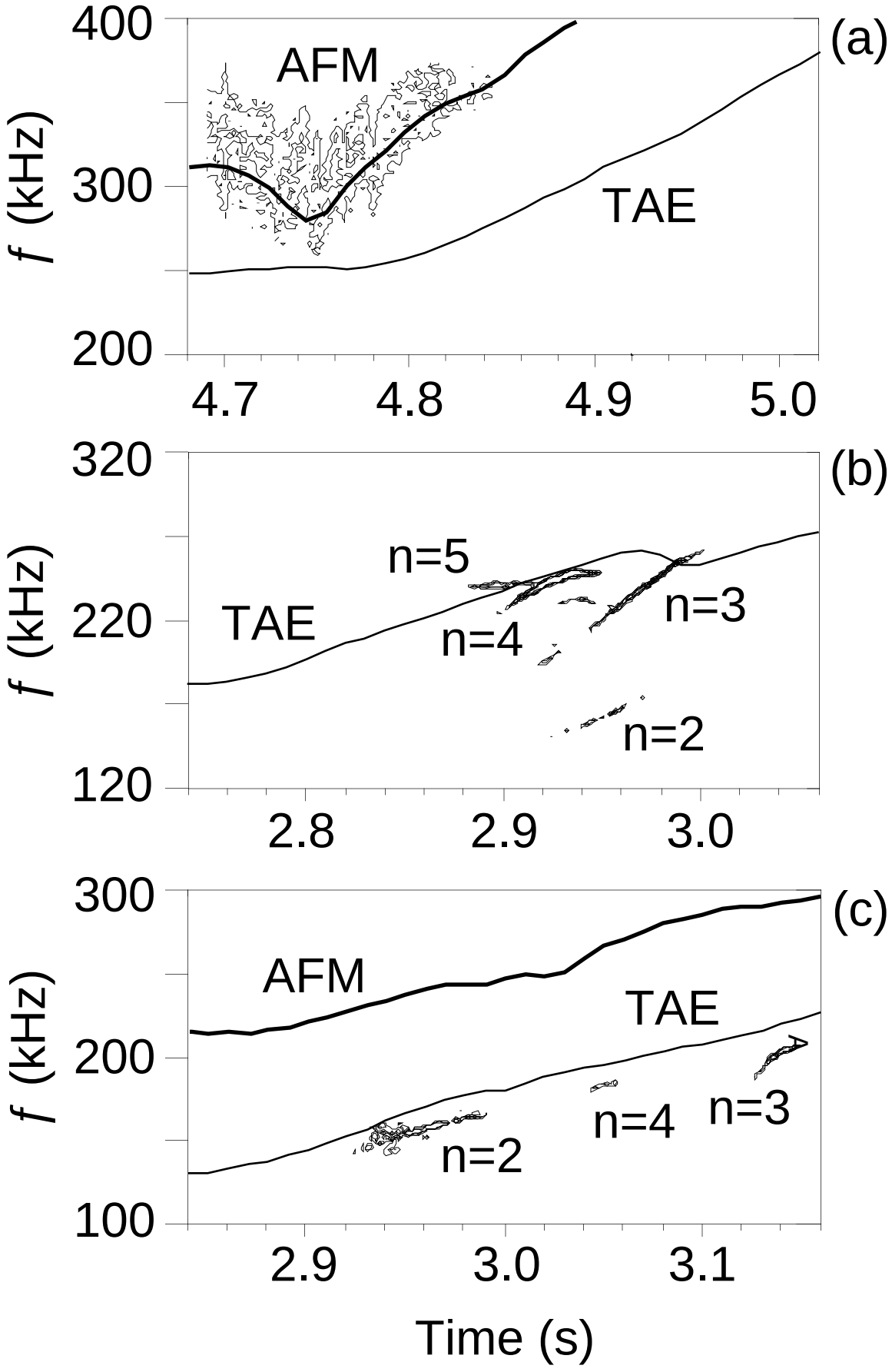

#94388, #103101, #89725

PPPL-3279/Figure 3

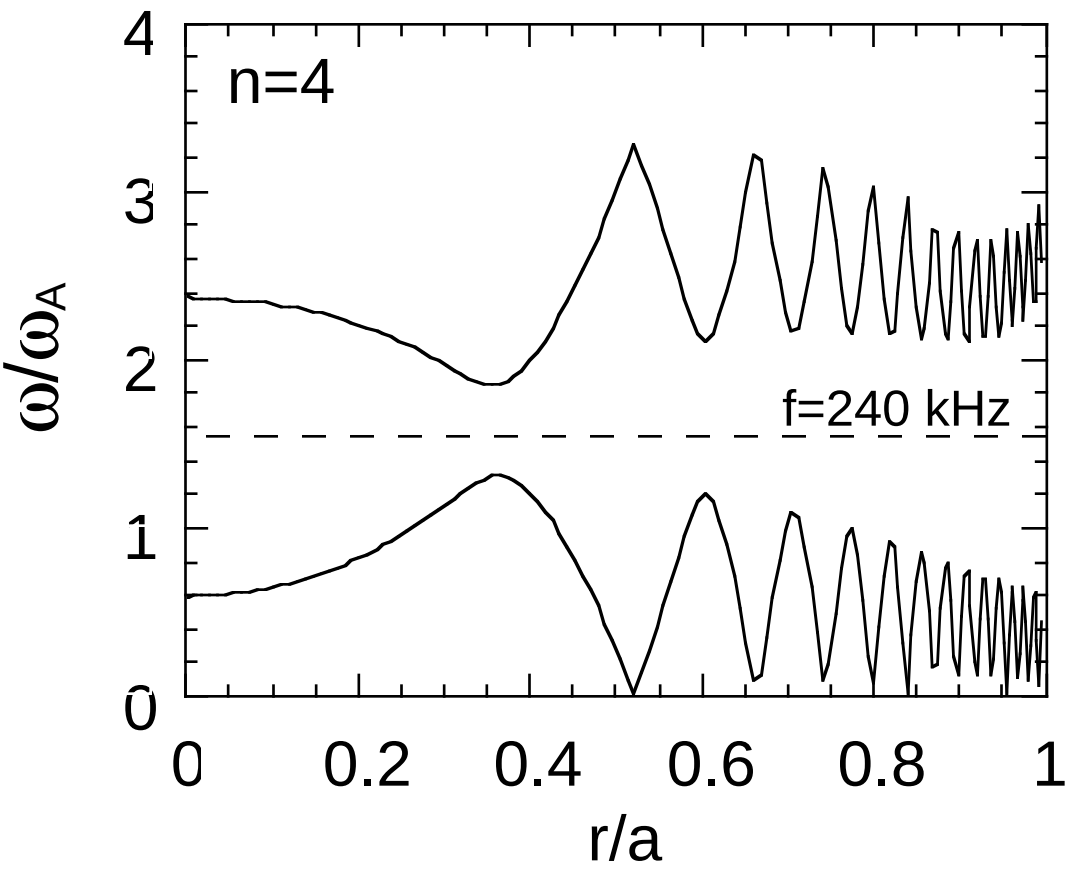

PPPL-3279/Figure 4

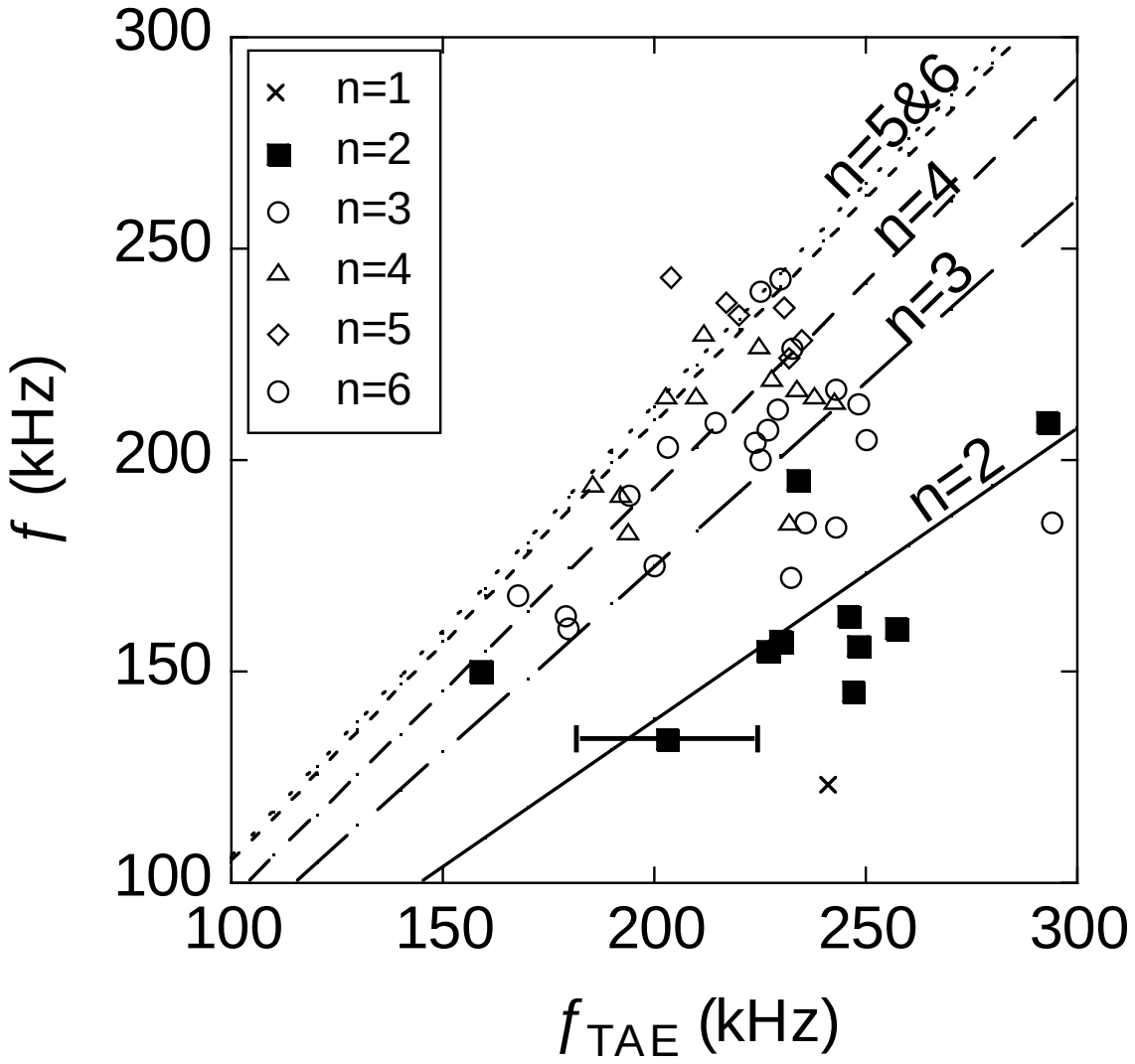

PPPL-3279/Figure 5

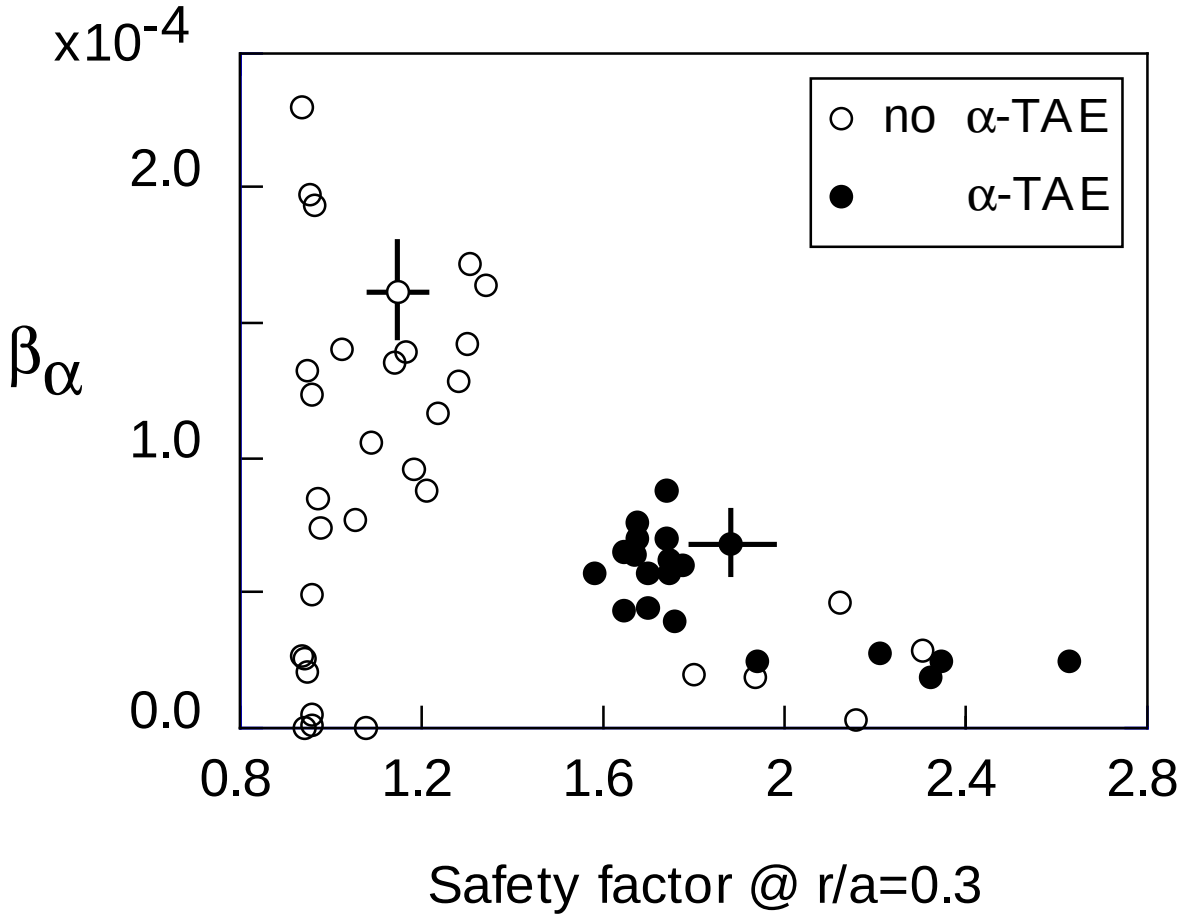

PPPL-3279/Figure 6

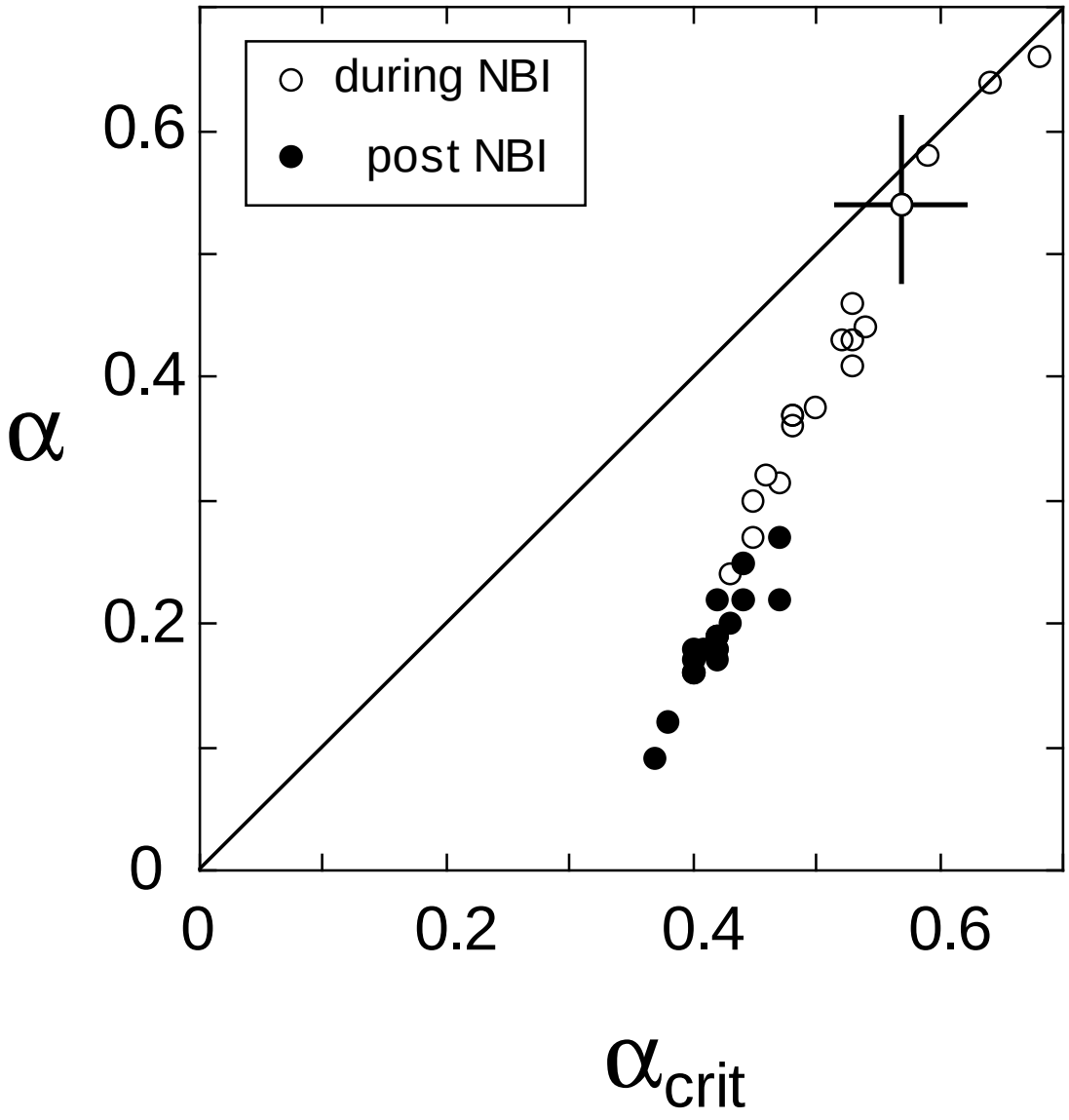

PPPL-3279/Figure 7

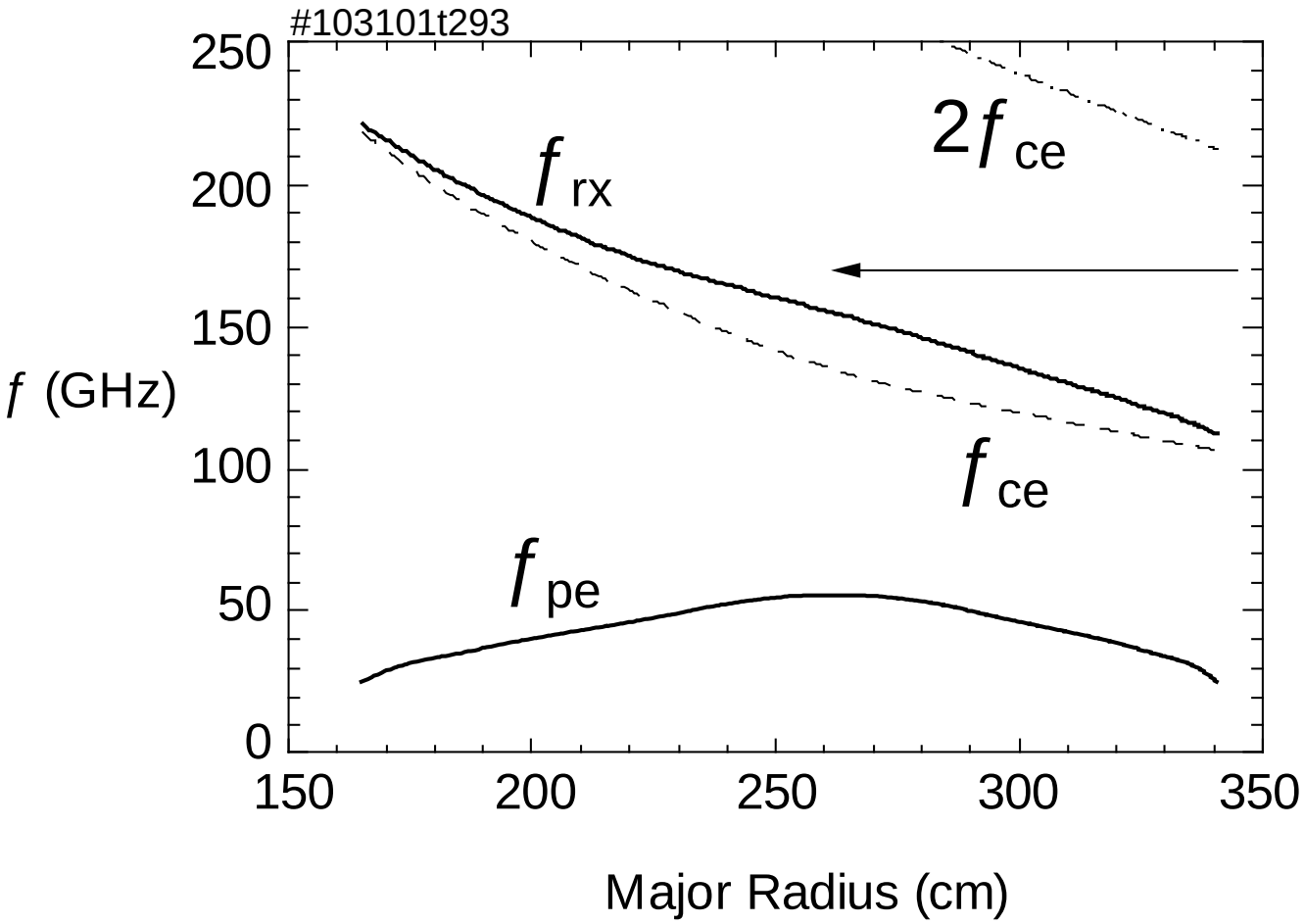

PPPL-3279/Figure 8

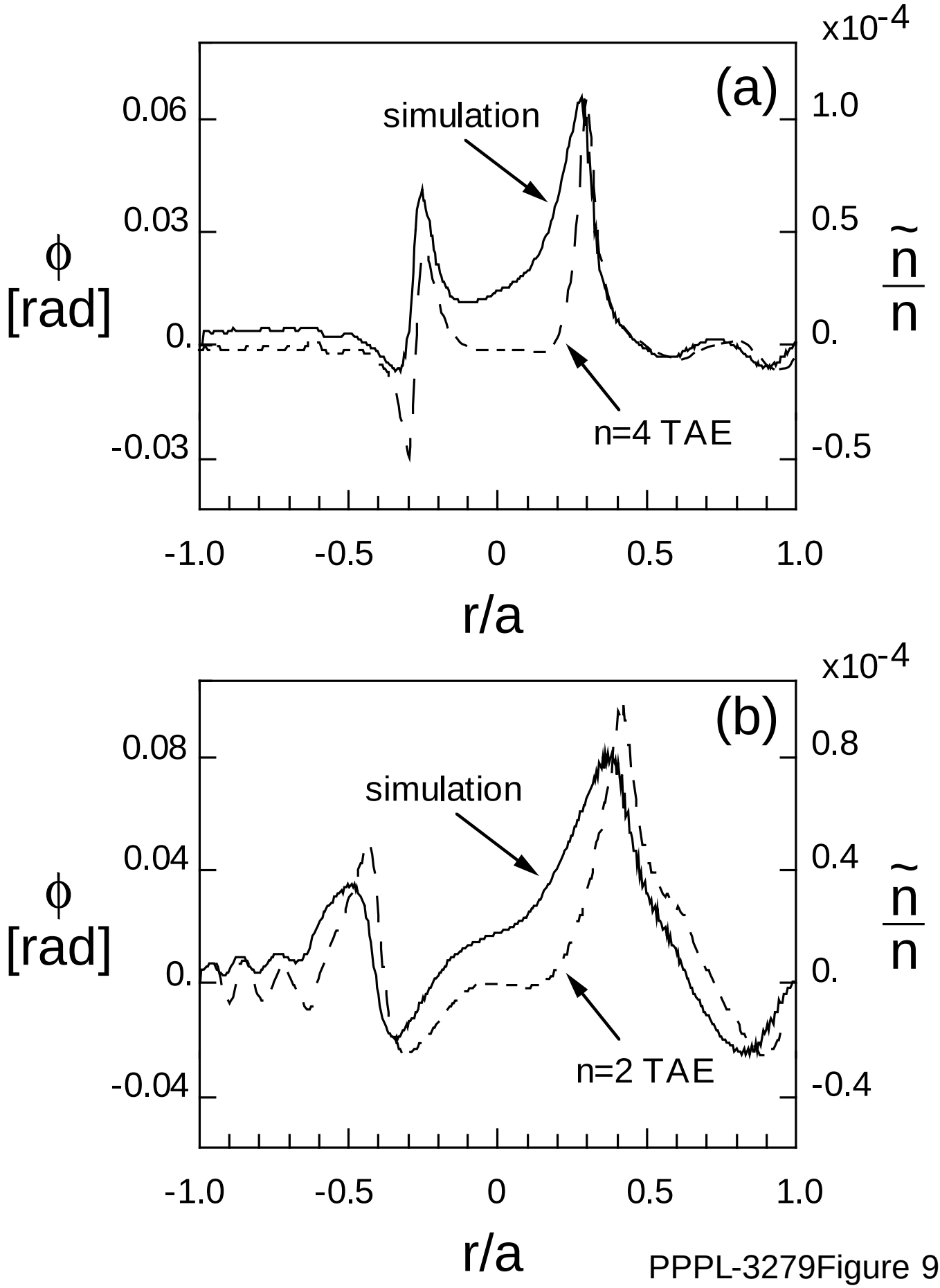

PPPL-3279Figure 9

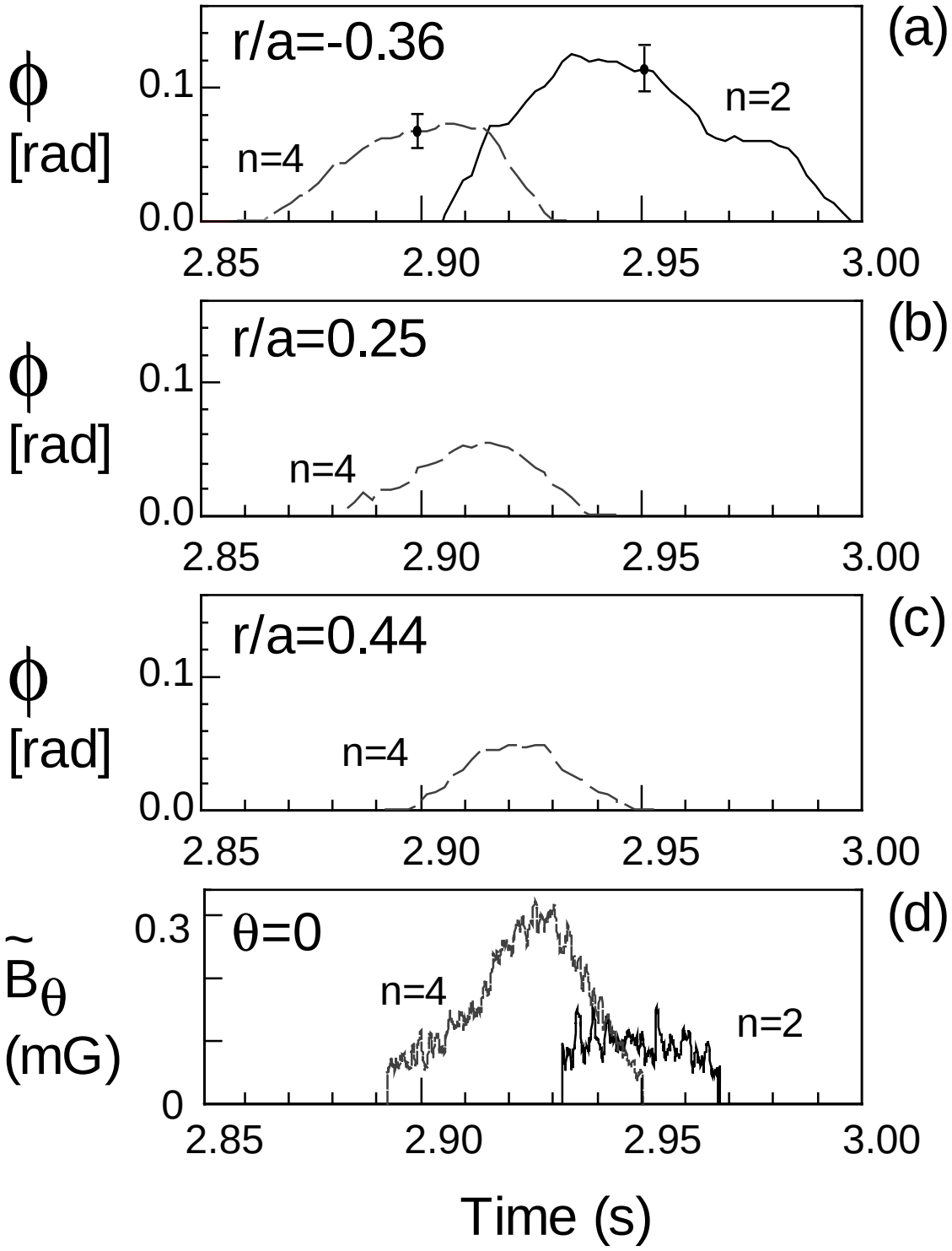

#103101: R=228, R=284, R=300 PPPL-3279/Figure 10

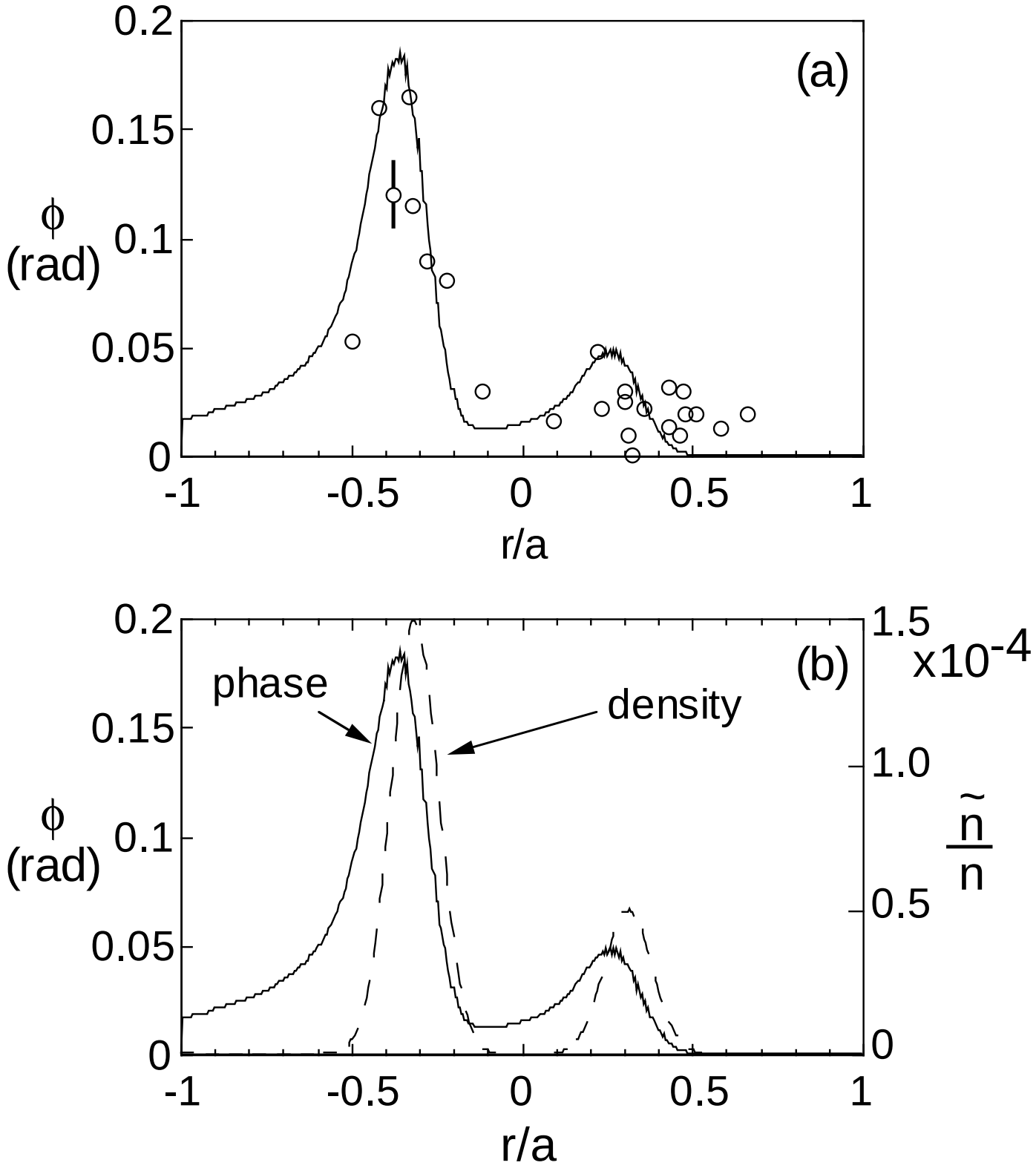

PPPL-3279/Figure 11

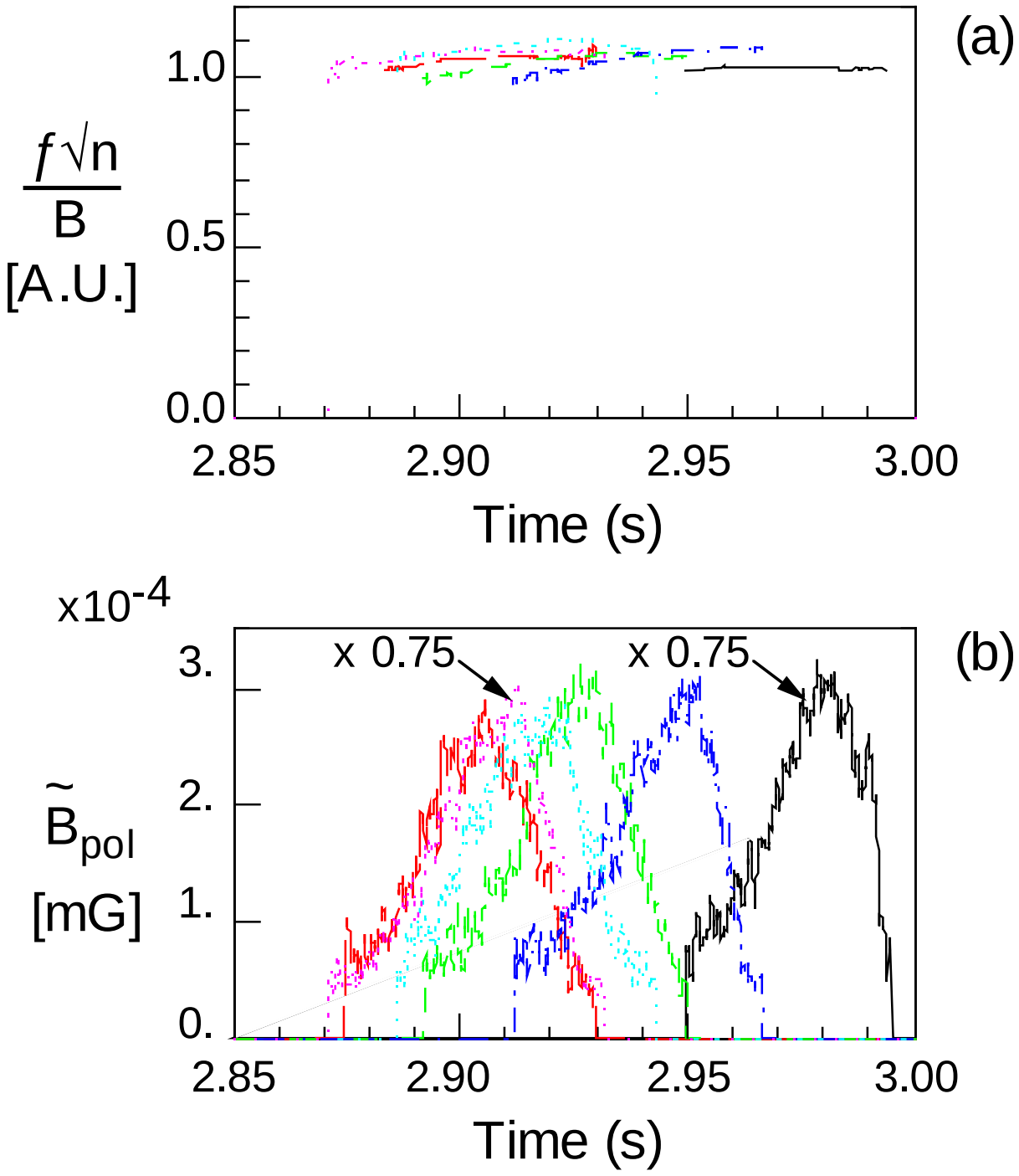

PPPL-3279/Figure 12

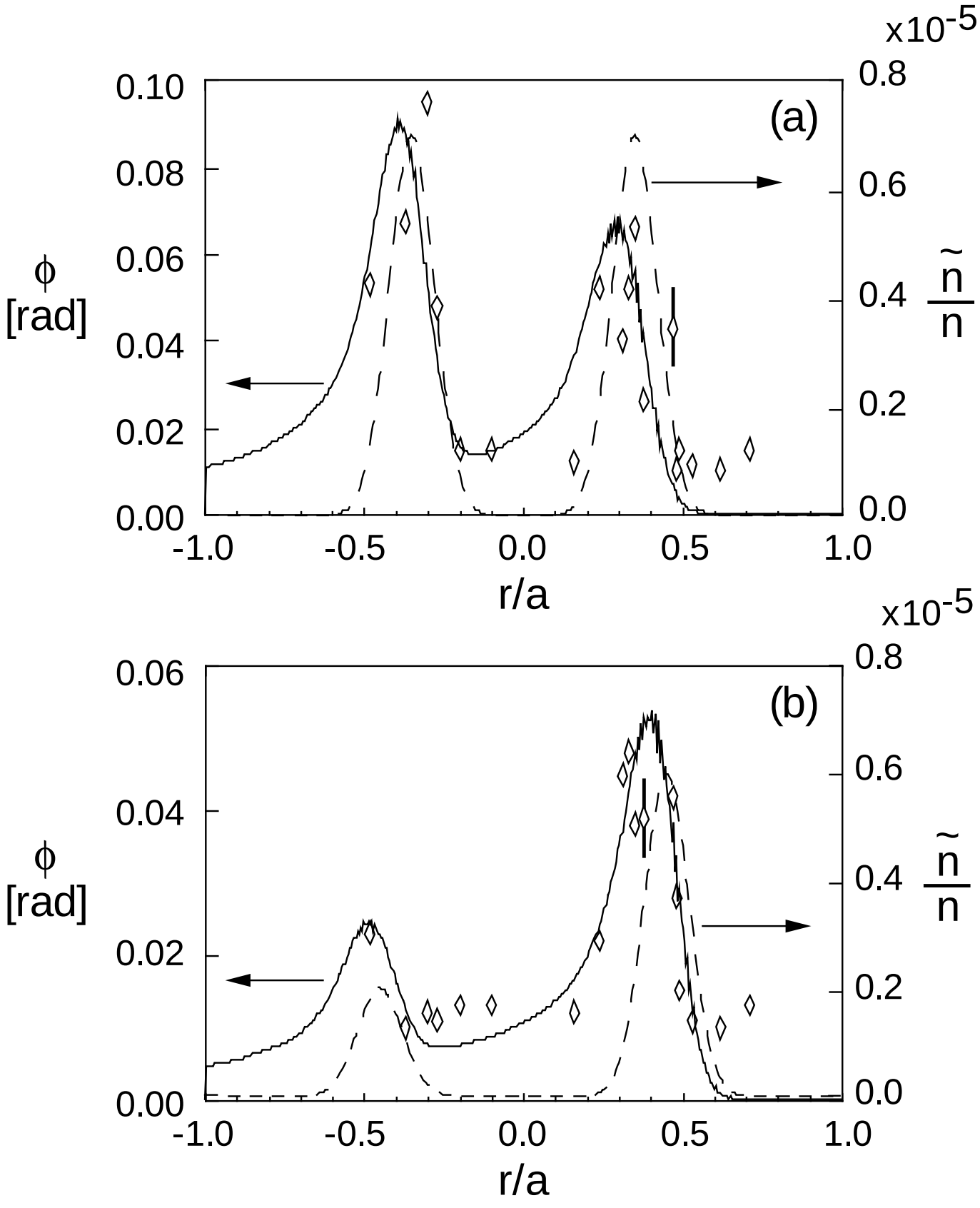

PPPL-3279/Figure 13

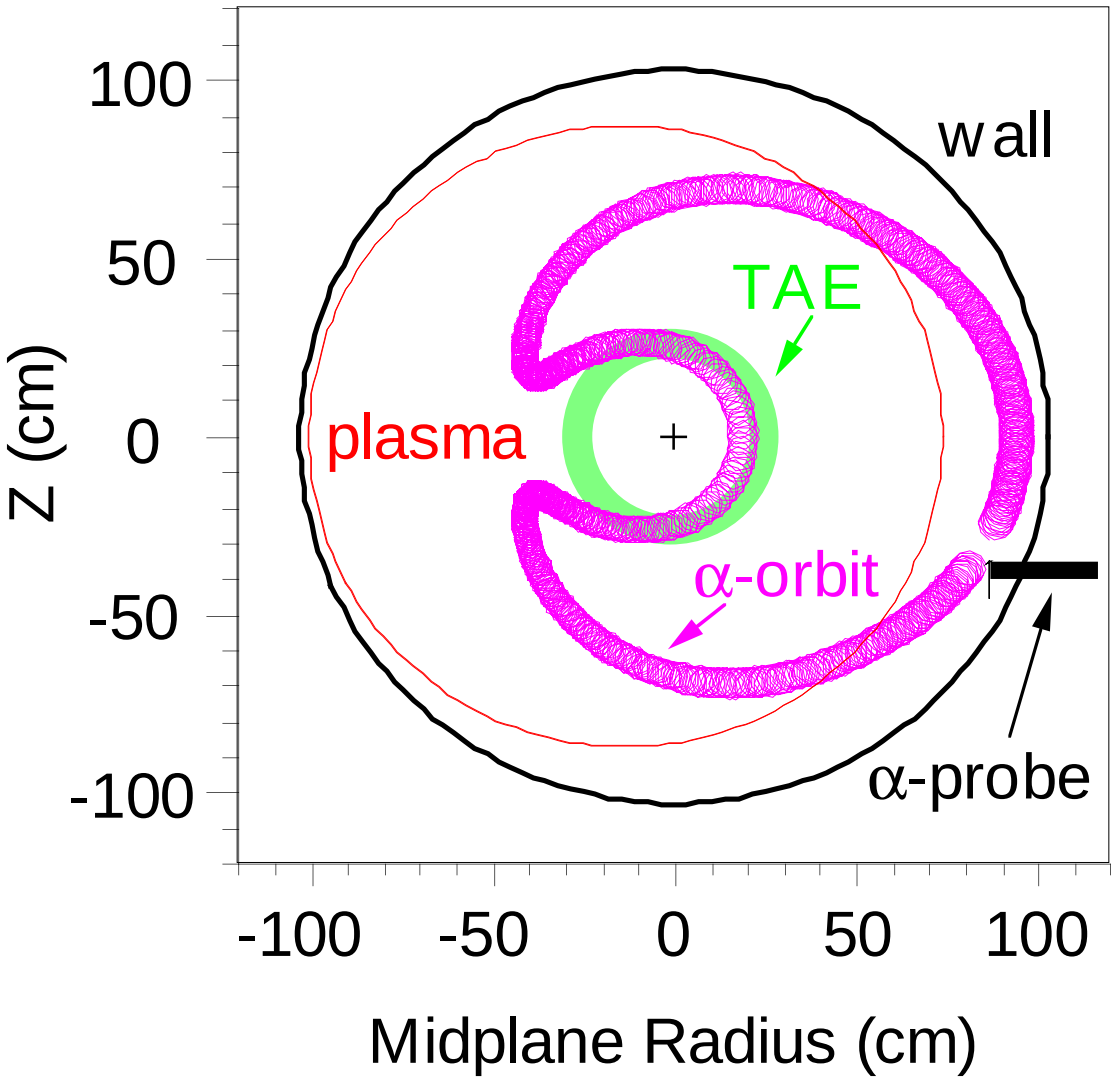

PPPL-3279/Figure 14

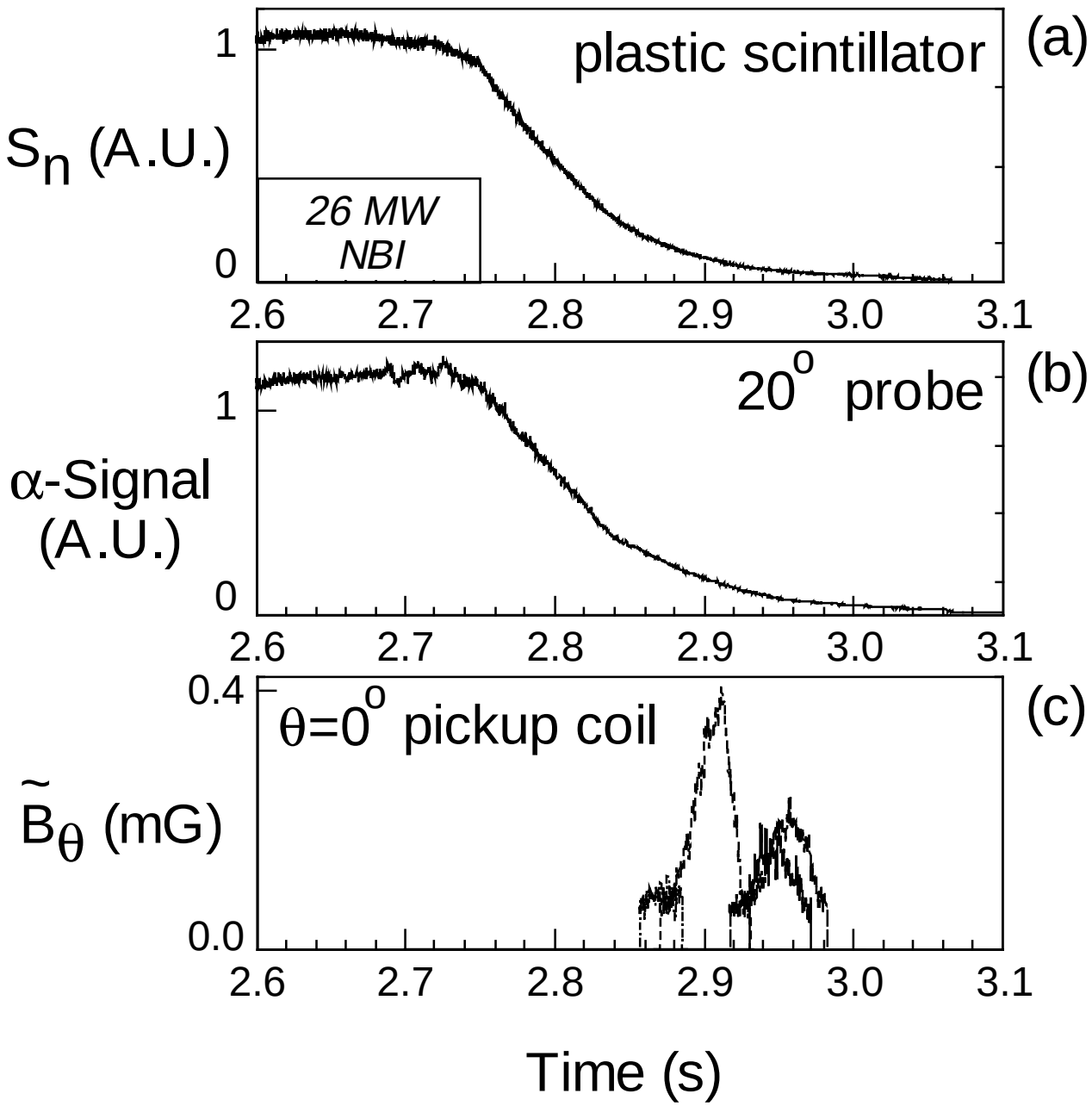

PPPL-3279/Figure 15